Supporting Information

Zhuang et al. 10.1073/pnas.1215176110

SI Results

Structural Integrity of Arrestin-1 in Various Media as Determined by Near-UV CD Spectroscopy. Arrestin-1 has 16 phenylalanines, 1 tryptophan, and 14 tyrosines, all of which contribute to its near-UV CD spectrum. The spectrum of arrestin-1 in native conformation in neutral buffer exhibits pronounced negative signals in the 270–290 nm range, whereas the spectrum of denatured protein in 8 M urea is near zero in this range (Fig. S1). We found that the presence of dodecylphosphocholine (DPC) or lyso-myristoylphosphatidylcholine (LMPC) micelles induced rapid precipitation of arrestin-1. Near-UV CD spectra were compared for arrestin-1 under native conditions (Fig. S1, red spectra), upon denaturing with 8 M urea (Fig. S1, green spectra), and in the presence of different membrane mimics. In the presence of 0.1% lyso-myristoylphosphatidylglycerol (LMPG) or amphipols (Fig. S1 *B* and *C*), CD spectra that are vaguely similar to that of arrestin-1 under physiological conditions were obtained, but significant loss of CD signal intensity in the 260–290 nm range was observed, suggestive of destabilization of ordered tertiary structure. In the presence of 0.2% β-n-decylmaltoside (DM) micelles, the CD spectral intensity from 265 to 290 nm actually increased, suggestive of a change or enhancement of tertiary structure. In contrast, three different types of bicelles (Fig. 1*A*) yielded CD spectra that were very similar to the spectrum of arrestin-1 under physiological conditions. These three bicelle systems were: (*i*) purely zwitterionic 2.5% (wt/vol) dimyristoylphosphatidylcholine + diheptanoylphosphatidylcholine (DMPC/D7PC) bicelles (q = 0.3, where q is the lipid-to-detergent mole:mole ratio, D7PC being the detergent component); (*ii*) net negatively charged 2.5% (wt/vol) DMPC/D7PC bicelles with 20 lipid-mol% dimyristoylphosphatidylglycerol (DMPG) (DMPC:DMPG = 4:1, q = 0.3); and (*iii*) positively charged 2.5% DMPC/D7PC bicelles with 20 lipid-mol % hexadecyltrimethylammonium bromide (HTAB) (DMPC:HTAB = 4:1, q = 0.3). Arrestin-1 was equally structurally-ordered in all three bicelle systems (Fig. 1*A*), identifying isotropic bicelles as a suitable medium for solution NMR-based studies of arrestin-1/rhodopsin interactions.

NMR Confirms the Release of Arrestin-1 C-Tail upon Rhodopsin Binding. Both limited proteolysis (1) and electron paramagnetic resonance (EPR) distance measurements (2, 3) indicated that the C-tail of arrestin-1 undergoes major conformational change upon receptor binding. To confirm the structural nature of these changes we collected NMR paramagnetic-relaxation enhancement (PRE) data to provide additional insight. A nitroxide spin label was introduced at site 16 of arrestin-1 and its impact on the intensities (reflected in line widths) of the C-tail NMR resonances was measured before and after binding to phosphorylated light-activated rhodopsin (P-Rh*) (Table S1). In free arrestin-1 the spin label induced significant line broadening for most of the C-tail resonances, indicating that they reside within 25 Å of the side chain of residue 16. However, little or no spin label-induced line broadening was detected following P-Rh* binding, indicating the backbone amides of the C-tail are now more than 25 Å away from the spin label. This result is consistent with the previous finding that the negatively charged C-tail is displaced from its basal association with the basic region in the N domain (4).

SI Methods

Preparation and Spin-Labeling of the I16C Mutant Form of Arrestin-1. A single cysteine was inserted at position 16 (I16C) of the oligomerization-resistant cysteine-less arrestin-1 mutant (C63A, C128S, C143S, F85A, and F197A) using a Qiagen Quickchange kit. The forward primer was 5′-CCACGTCATCTTTAAAAA-GTGCTCCCGTGATAAATCGGTGACC-3′ and the reverse primer was 5′-GGTCACCGATTTATCACGGGAGCACTTT-TTAAAGATGACGTGG-3′. Purified arrestin-1 samples were stored for short periods at 4 °C in Tris buffer (25 mM Tris pH 7.5, 150 mM NaCl, 5 mM DTT, and 1 mM EDTA) and frozen at –80 °C for long-term storage. NMR samples were prepared by changing the buffer to Bis•Tris (25 mM Bis•Tris, 100 mM NaCl, 5 mM DTT, and 0.1 mM EDTA pH 6.5) using an ultrafiltration concentrator [Millipore; molecular weight cut-off (MWCO) = 30 kDa].

For spin labeling of the I16C arrestin-1 single-cysteine mutant, DTT was removed by exchanging the buffer to a degassed reductant-free Bis•Tris solution (25 mM Bis•Tris, 100 mM NaCl, and 0.1 mM EDTA pH 6.5) using a centrifugal ultrafiltration cartridge (Millipore; MWCO = 30 kDa). Protein samples were then diluted using reductant-free Bis•Tris buffer to a final concentration of 0.5 mg/mL, followed by mixing with a 10-fold molar excess of the sulfhydryl-specific spin label reagent 2,2,5,5-tetramethylpyrroline-3-yl-methanethiosulfonate (MTSL; Toronto Research Chemical). The mixture was incubated under argon covered with aluminum foil at 4 °C overnight and the unreacted MTSL was removed by buffer exchange using centrifugal ultrafiltration (Millipore filter, MWCO = 30 kDa). The final NMR sample was prepared in the reductant-free Bis•Tris solution, maintaining a low arrestin-1 concentration (30–50 μM) to minimize dimerization. Following collection of a transverse relaxation optimized spectroscopy (TROSY) NMR spectrum, the paramagnetic spin label was reduced to its diamagnetic form by adding ascorbic acid to 5 mM and incubating at 37 °C for 2 h. This process was followed by collection of another TROSY NMR spectrum using identical parameters used for the paramagnetic sample. Both paramagnetic and diamagnetic samples were also subjected to continuous wave EPR spectroscopy to confirm the completeness of spin-labeling and of reduction to the diamagnetic form, respectively. Typically, the spin labeling efficiency was >95%, with the efficiency of reduction being ~100%.

Preparation of Rhodopsin, Phosphorylated Rhodopsin, and Phosphorylated Opsin in Bicelles. The preparation of phosphorylated rhodopsin (P-Rh) includes four major steps: isolation of retinal outer segments (ROS), phosphorylation, regeneration, and urea stripping. All operations were carried out under dim red light unless otherwise indicated. ROS were enriched by sucrose gradient from 50 frozen bovine retinas (purchased from W. L. Lawson Co.) as previously described (5). After sonication, the ROS pellet was resuspended in 100 mM potassium phosphate buffer (pH 7.4) to a final rhodopsin concentration of 0.5 mg/mL. The rhodopsin suspension was incubated under bright light for 240 min in the presence of 3 mM ATP, 3 mM GTP, and 5 mM $MgCl_2$ to initiate rhodopsin phosphorylation by endogenous G protein-coupled receptor kinase 1 (GRK1; also known as rhodopsin kinase). This process yielded rhodopsin with high phosphorylation levels (6), which ensures high-affinity arrestin binding (7). Rhodopsin was fully regenerated by 11-*cis*-retinal (two additions of threefold molar excess) in 100 mM potassium phosphate buffer, pH 7.4, supplemented with 2% (wt/vol) BSA, 1 mM $MgCl_2$, and 0.5 mM EDTA for 1 h at room temperature (5). After regeneration, 5 M urea was added to remove peripherally associated soluble proteins from the membranes and the

pellets were washed five times with 50 mM Tris•HCl, pH 7.5, 1 mM EDTA, and resuspended in this buffer.

For solubilization with bicelles, regenerated rhodopsin was pelleted by centrifugation at 14,000 × *g* for 30 min and solubilized by the addition of 12.5% (wt/vol) anionic bicelles ($q = 0.3$, DMPC: DMPG = 4:1) and incubated for 2 h at 0 °C. The sample was centrifuged at 14,000 × *g* for 30 min to remove insoluble material. The concentration of dark P-Rh was measured by light absorption at 500 nm (mol extinction coefficient is 40,600 $M^{-1}{\cdot}cm^{-1}$) using an Olis DW2000 dual-beam spectrophotometer adapted for a dark room. A typical rhodopsin reconstitution was performed by mixing 150 μL 12.5% (wt/vol) anionic bicelles with ROS membrane containing 3 mg rhodopsin. The recovery of rhodopsin was around 90% and the final bicelle concentration was kept within a 6–8% range. The amount of the native lipids solubilized from ROS membranes were considered to be negligible as assessed by 1D proton NMR spectroscopy.

Rhodopsin in bicelles was prepared as described for P-Rh, but without the rhodopsin phosphorylation step and subsequent regeneration. Dark nonphosphorylated rhodopsin in ROS was solubilized with bicelles and mixed with arrestin-1. To generate the light-activated Rh* and P-Rh*, the samples were bleached under bright light until the absorbance peak at ~500 nm completely disappeared. Because of the high concentration of rhodopsin in samples complete bleaching required a number of hours (overnight). Therefore, we cannot exclude the formation of other photoproducts in addition to Meta II, including opsin. However, because rhodopsin was bleached in the presence of arrestin-1, which is known to stabilize Meta II similar to transducin, and because even the C-terminal transducin peptide shifts the opsin conformation into an active Meta II-like state, the arrestin-rhodopsin complexes can be safely assumed to resemble those formed with corresponding light-activated rhodopsin species.

Phosphorylated opsin (P-opsin) was prepared by bleaching P-Rh containing membranes overnight with 200 mM hydroxylamine (NH_2OH) under bright light before it was solubilized with bicelles. The 11-*trans*-retinal and excess hydroxylamine were removed from ROS membranes by centrifugation at 14,000 × *g* for 30 min. Then, 5 mM hydroxylamine was added to the final sample to prevent regeneration of light-sensitive P-Rh by remaining traces of 11-*cis*-retinal.

Near-UV CD (250–320 nm) Spectroscopy to Identify Model Membrane Conditions that Preserve Native Arrestin-1 Structure. Near-UV CD spectra are sensitive to the overall tertiary structure of proteins, yielding significant signals from well-ordered aromatic amino acid side chains and disulfide bonds. All near-UV CD spectra of arrestin-1 were acquired at 25 °C using a Jasco J-810 CD spectropolarimeter over the wavelength range of 250–320 nm. A masked cell (1-cm pathlength) with a minimum volume of 500 μL was used to acquire CD spectra. Five scans were averaged for each sample to achieve desirable signal-to-noise. Spectra were baseline-corrected by subtracting the CD spectrum of the buffer. A reference spectrum for well-folded arrestin-1 was acquired using 50 μM arrestin-1 in Bis•Tris buffer (25 mM Bis•Tris, 100 mM NaCl, 0.1 mM EDTA, and pH 6.5). A spectrum of unfolded arrestin-1 was also obtained for 50 μM arrestin-1 in the same buffer plus 8 M urea. Near-UV spectra of 50 μM arrestin-1 were also obtained in the presence of detergents: (*i*) 0.1% LMPG and (*ii*) 0.2% DM. Bicelle mixtures tested were: (*i*) zwitterionic: 2.5% (wt/vol) D7PC/DMPC, $q = 0.3$ (mole ratio D7PC:DMPC = 3.3:1); (*ii*) anionic: 2.5% DMPC/D7PC/ DMPG (DMPC:DMPG = 4:1) $q = 0.3$ [D7PC:(DMPC+DMPG) = 3.3:1]; and (*iii*) cationic: 2.5% (wt/vol) DMPC/D7PC/ HTAB (DMPC:HTAB = 4:1) $q = 0.3$ [D7PC:(DMPC+HTAB)=3.3:1]. Amphipathic polymers ("amphipols") tested were: (*i*) 0.2% PMAL-C8, (*ii*) 0.2% PMAL-C12, and (*iii*) 0.2% PMAL-C16.

Near-UV CD spectra were acquired after the proteins had been premixed with detergents, bicelles or amphipols for 4–5 d at room temperature. Detergents and amphipols were purchased from Anatrace-Affymetrix, and lipids were purchased from Avanti Polar Lipids.

Preparation of Arrestin-1 That Is Perdeuterated Except for Side-Chain Methyl Groups of Leucine, Isoleucine, and Valine, Which Are also ^{13}C-Labeled. Precursors "A" (α-ketovaleric acid salt, 3-methyl-^{13}C, 3,4,4,4-D_4) and "B" (α-ketobutyric acid salt, methyl-^{13}C, 3,3-D_2) were purchased from Cambridge Isotopes (catalog nos. CDLM-7317–0 and CDLM-7318–0, respectively).

Escherichia coli cells harboring an inducible plasmid that encodes the F85A/F197A (tetramerization-resistant) mutant form of arrestin-1 were used to inoculate 5 mL of a Luria broth (LB) prepared using D_2O. The cell were grown overnight at 37 °C. From these cultures we then removed 50 μL and inoculated 5–10 mL of minimal medium that contains perdeuterated glucose and D_2O. Cultures were then grown at 30 °C until culture appeared turbid. Each 5-mL culture was then used to inoculate 500 mL (or 1L) of minimal medium that contains perdeuterated glucose, D_2O, and precursors A and B (above). Cultures were shaken at 30 °C until OD_{600} reached 0.6, at which point additional precursors were added (additional A to 75 mg/L and B to 45 mg/L). Shaking of cultures was then continued for 30 min at which point isopropyl-β-D-thiogalactopyranoside (IPTG) was added to 25 μM to induce expression of arrestin-1. Shaking was then continued for 18 h, followed by cell harvesting. Labeled arrestin-1 was then purified and prepared for NMR using the standard procedure.

NMR Experiments. NMR experiments were performed using Bruker Avance 800-MHz and 600-MHz spectrometers equipped with cryogenic triple resonance probes with *z*-axis pulse-field gradients. A sensitivity-enhanced, phase-sensitive TROSY pulse sequence was used to acquire all ^1H-^{15}N correlated 2D spectra (8). Because of the low concentration of the arrestin-1 samples used in this study (30–50 μM), most NMR spectra were acquired using 2,048 × 128 complex points with 200 scans per increment, which result in a typical 20-h acquisition time. For samples containing ^{15}N-arrestin-1 in the presence of excess Rh* or P-Rh*, we conducted experiments in which 2-h TROSY spectra were collected before and after 20-h data collection. In the case of both complexes, the intensity of the arrestin-1 peaks in the 2-h TROSY spectra collected after the 20-h run were weaker than before the 20-h run. Average loss of peak intensity was about 40% for the Rh* complex and about 70% for the P-Rh* complex. However, with only a few exceptions, new peaks did not appear in the "after" spectra relative to the "before" spectra. This result suggests that the arrestin-1 complexes with Rh* or P-Rh* do undergo some sort of time-dependent loss of integrity (most likely formation of very large aggregates). Although this sample loss will attenuate peak intensities in the 20-h TROSY spectra reported in this article, this does not impact peak positions or impact the interpretation of these spectra as presented in the main text or *SI Text*.

All spectra were acquired at 308 K with temperature precalibrated using deuterated methanol. All NMR data were processed using nmrPipe (9) with Gaussian apodization, linear prediction, and zero filling. Peak intensities for determination of paramagnetic relaxation enhancements were measured using Sparky (10).

The 2D methyl-TROSY experiment was run using the ^1H,^{13}C-HMQC pulse sequence. The 1,024 × 512 complex points covering spectral widths of 14 × 22 ppm (^1H and ^{13}C, respectively) were acquired with 128 scans per each increment, which resulted in a 20-h acquisition time. The acquired spectra were processed with one-time zero filling with a squared sine-bell apodization function.

The 1:1 Binding Model for Fitting NMR Titration Data For the Arrestin-1 Complexes with P-Rh and Rh*. Binding of P-Rh and Rh* to arrestin-1 occurs on the rapid exchange time scale on the NMR time scale. Under conditions of rapid exchange, complex formation between molecules can result in changes in NMR peak positions for the observed molecule, which reflects the population-weighted average peaks between free and complexed populations. In this case, the observed change in chemical shift (or resonance frequency) in "molecule A" (arrestin-1) induced by complex formation with "molecule B" (P-Rh or Rh*) is:

$$\text{observed change in chemical shift} = [\text{B}]^* \text{ maximum change in chemical shift}/(\text{K}_\text{D} + [\text{B}]), \quad \textbf{[S1]}$$

where [B] is the free concentration of molecule B and the "maximum change in chemical shift" is the change in chemical shift that occurs when molecule A is fully saturated with molecule B. It is often reasonable to assume that the free B concentration equals the total (free + complexed) B concentration. However, that is not the case for the titrations of arrestin-1 (molecule A) with P-Rh (molecule B). In this case the following equation gives the free [B] concentration:

$$\text{free } [\text{B}] = \left\{ \text{total } [\text{B}]_\text{total} - [\text{A}]_\text{total} - \text{K}_\text{D} + \left[\left([\text{B}]_\text{total} - [\text{A}]_\text{total} - \text{K}_\text{D} \right)^2 + 4 * \text{K}_\text{D} * [\text{B}]_\text{total} \right]^{1/2} \right\} / 2 \quad \textbf{[S2]}$$

For nonlinear least-squares analysis, Eq. **S2** is plugged into Eq. **S1** and the resulting equation is then fit to the experimental data to obtain a best fit and estimates of K_D and the maximum change in chemical shift for the peak in question.

1. Palczewski K, Pulvermüller A, Buczyłko J, Hofmann KP (1991) Phosphorylated rhodopsin and heparin induce similar conformational changes in arrestin. *J Biol Chem* 266(28): 18649–18654.
2. Hanson SM, et al. (2006) Differential interaction of spin-labeled arrestin with inactive and active phosphorhodopsin. *Proc Natl Acad Sci USA* 103(13):4900–4905.
3. Vishnivetskiy SA, et al. (2010) The role of arrestin alpha-helix I in receptor binding. *J Mol Biol* 395(1):42–54.
4. Gurevich VV, Chen C-Y, Kim CM, Benovic JL (1994) Visual arrestin binding to rhodopsin. Intramolecular interaction between the basic N terminus and acidic C terminus of arrestin may regulate binding selectivity. *J Biol Chem* 269(12): 8721–8727.
5. Mcdowell JH (1993) *Methods in Neurosciences: Photoreceptor Cells* (Academic, San Diego, CA), pp 123–130.
6. Wilden U, Kühn H (1982) Light-dependent phosphorylation of rhodopsin: Number of phosphorylation sites. *Biochemistry* 21(12):3014–3022.
7. Vishnivetskiy SA, et al. (2007) Regulation of arrestin binding by rhodopsin phosphorylation level. *J Biol Chem* 282(44):32075–32083.
8. Weigelt J (1998) Single scan, sensitivity- and gradient-enhanced TROSY for multidimensional NMR experiments. *J Am Chem Soc* 120(48):10778–10779.
9. Delaglio F, et al. (1995) NMRPipe: a multidimensional spectral processing system based on UNIX pipes. *J Biomol NMR* 6(3):277–293.
10. Goddard TD, Kneller DG (2008) Sparky 3. (University of California, San Francisco). Available at http://www.cgl.ucsf.edu/home/sparky/. Accessed Dec. 20, 2012.

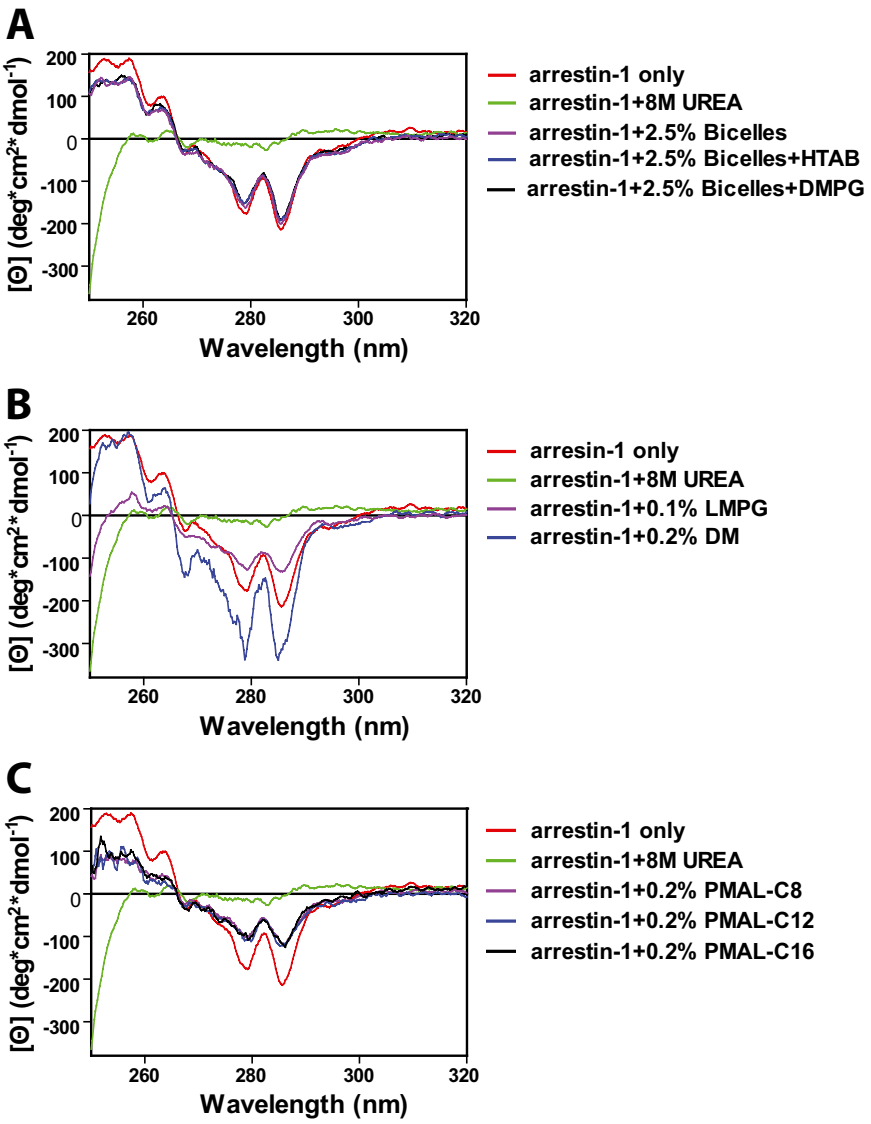

Fig. S1. Near-UV CD spectra of arrestin-1 in the presence of NMR-compatible model membranes. (*A*) Arrestin-1 (50 μM) samples were prepared in zwitterionic bicelles (purple), cationic bicelles (blue), and anionic bicelles (black). The reference spectrum for a sample in buffer is colored in red. The spectrum of denatured arrestin-1 in 8 M urea is colored in green. Exact sample compositions are described in *SI Methods*. (*B*) The reference spectrum for a sample in buffer-only is colored in red. The spectrum of denatured arrestin-1 in 8 M urea is colored in green. Spectra of arrestin-1 in detergent micelles composed of LMPG (purple) or DM (blue). (*C*) Spectra of arrestin-1 in zwitterionic amphipols composed of PMAL-C8 (purple), PMAL-C12 (blue), and PMAL-C16 (black). All samples contained 50 μM arrestin-1 at pH 6.5 and 298 K.

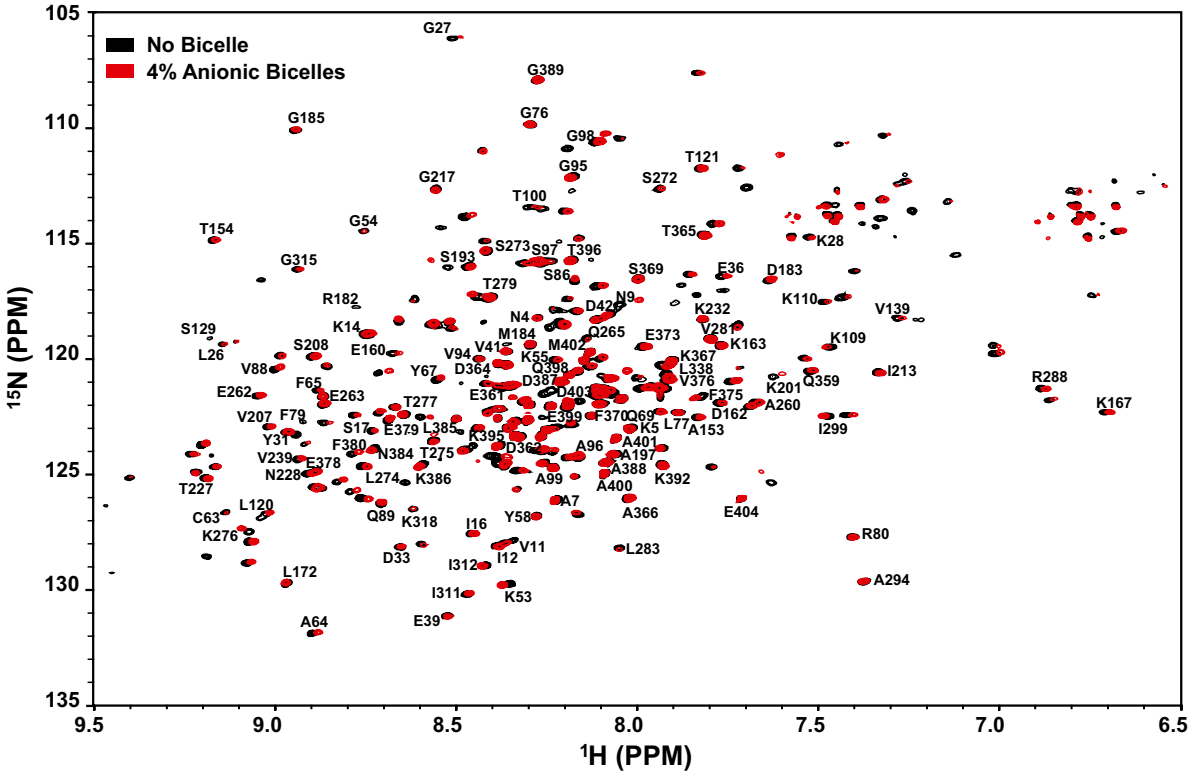

Fig. S2. ^{1}H,^{15}N-TROSY NMR spectra of uniformly-^{2}H,^{15}N-labeled arrestin-1 in the absence (black) and presence (red) of 4% (wt/vol) anionic bicelles. Samples were prepared in 10% D_2O (in H_2O) containing 25 mM Bis•Tris, 100 mM NaCl, 0.1 mM EDTA, and 5 mM DTT, pH 6.5. Under these conditions all amide protons had been back-exchanged from ^{2}H to ^{1}H. Both spectra were acquired at 308 K.

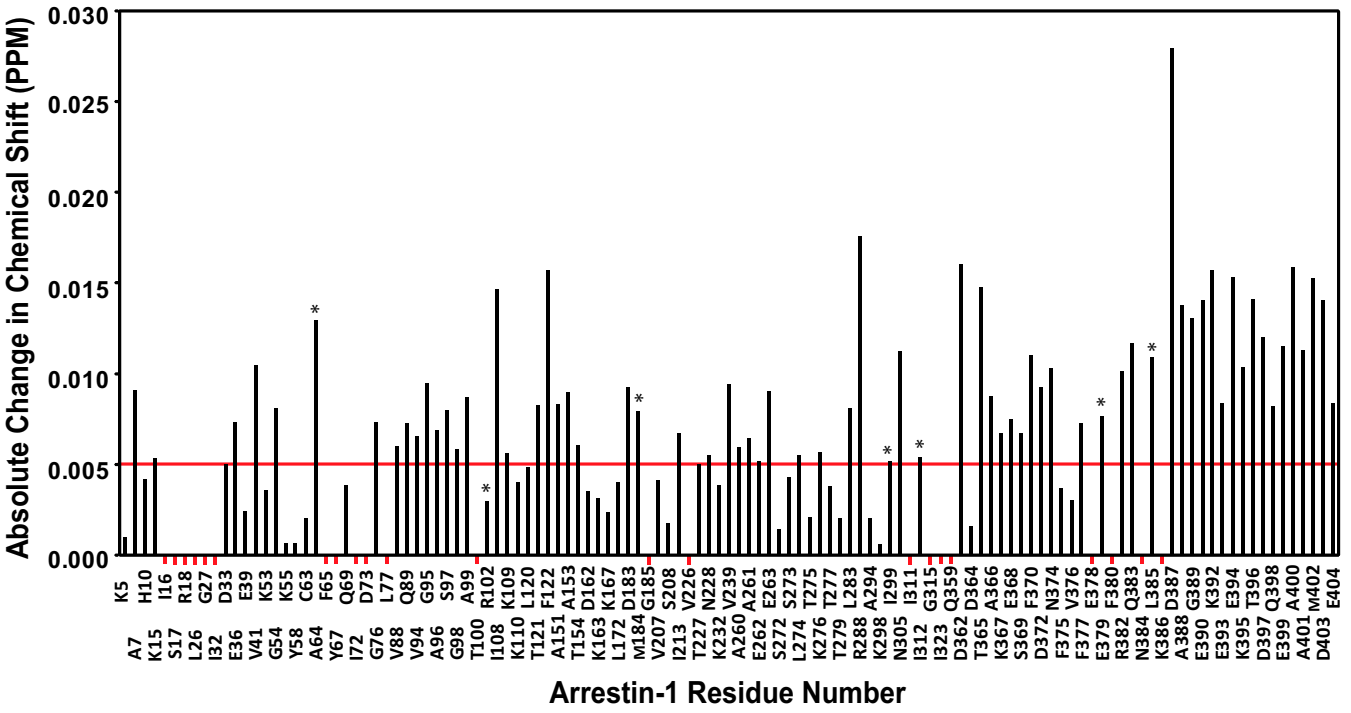

Fig. S3. Absolute values of changes in TROSY resonance chemical shifts induced by binding of P-Rh to arrestin-1 at 1:2 arrestin-1:P-Rh (mole:mole). At a 1:4 arrestin-1:P-Rh ratio many additional peaks broaden beyond detection (Fig. 1*A*). Assigned sites where arrestin-1 peaks disappeared in the presence of P-Rh are indicated by a small, negative red bars, whereas sites for which the binding of P-Rh induced significant line broadening are marked with asterisks. The horizontal red line is the cut-off for statistical significance (changes higher than 0.010 ppm were considered to be significant). The samples contained 30 μM $^{2}H,^{15}N$-labeled arrestin-1 ± P-Rh in 4.2% (wt/vol) anionic bicelles, 25 mM Bis•Tris, 100 mM NaCl, 0.1 mM EDTA, 5 mM DTT pH 6.5 at 308 K. The bicelles in all samples in this work contained DMPC:DMPG = 4:1 (mol:mol), q = 0.3, where q is the mol:mol ratio of the detergent-like D7PC to DMPC+DMPG.

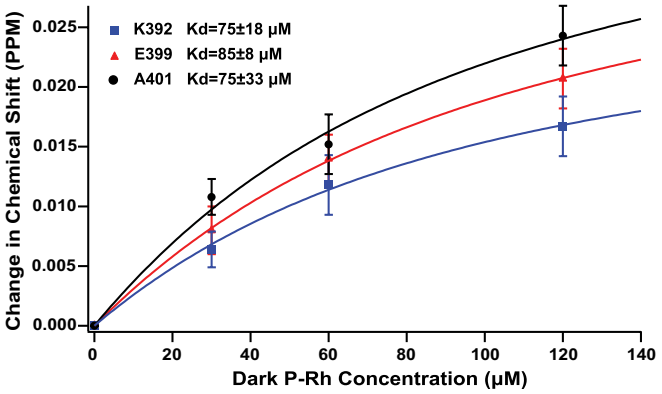

Fig. S4. Estimation of K_D for binding of arrestin-1 to dark state P-Rh. Changes in the TROSY NMR chemical shifts of arrestin-1 (Fig. 1*A*) for the resonances from K392 (blue), A401 (black), and E399 (red) were plotted as a function of the P-Rh concentration. The K_D for each curve was determined by fitting the model for 1:1 noncooperative binding to the data using nonlinear least squares analysis (see Eqs. **S1** and **S2**). Based on the three individual fits, the K_D is estimated as 80 ± 30 μM.

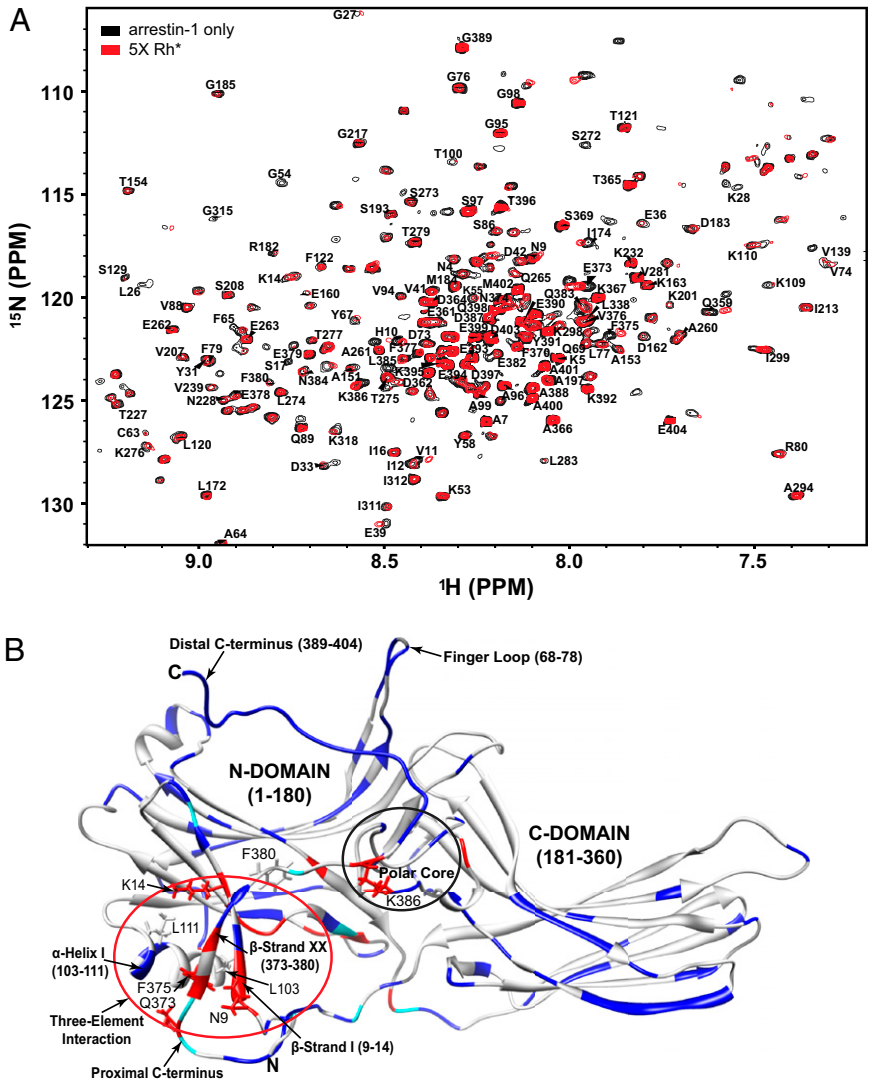

Fig. S5. Arrestin-1 binding to Rh*. TROSY spectra of 30 μM ^{2}H,^{15}N-labeled arrestin-1 were acquired in the presence of bicelles containing varying Rh*. (*A*) (black spectrum) Arrestin-1 in absence of Rh*. Only very small chemical-shift changes were observed in the presence of a fivefold molar excess of Rh* (red spectrum). (*B*) Mapping of Rh*-induced site-specific NMR chemical-shift changes onto the 3D structure of arrestin-1 (PDB ID 1CF1). Red sites are those for which the backbone amide chemical shifts changed by 0.010 ppm or more. Light-blue sites are those for which peaks shifted by less than 0.010 ppm, but underwent significant line-broadening in response to Rh*. Resonances for dark blue sites neither shifted significantly nor broadened.

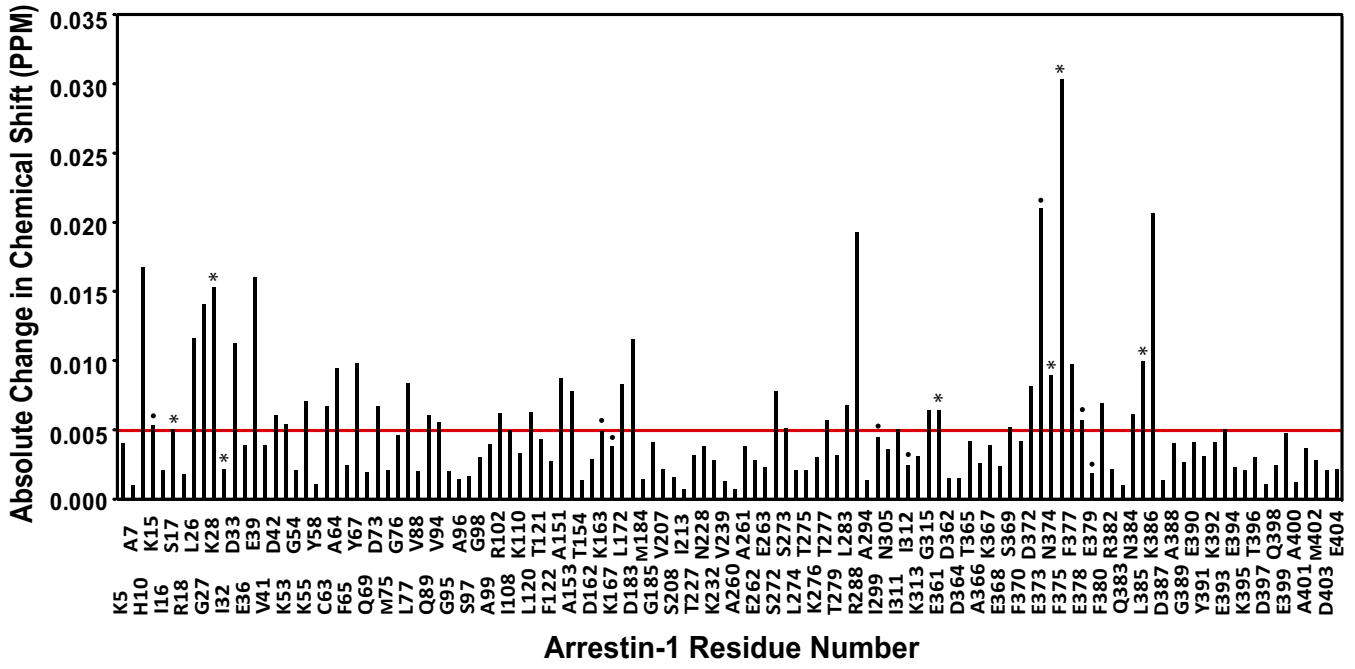

Fig. S6. Absolute values of the changes in arrestin-1 NMR chemical shifts for assigned residues induced by the presence of a fivefold molar excess of Rh*. The residues exhibiting significant line broadening are labeled with asterisks. The residues exhibiting significant line sharpening are labeled with dots. The horizontal red line is the cut-off for statistical significance (changes higher than 0.005 ppm were considered to be significant). As shown in Fig. S5*B*, TROSY spectra of 30 μM ^{2}H, ^{15}N-labeled arrestin-1 were acquired in the absence and presence of 5× Rh* (mole:mole) at 308 K. Samples contained 25 mM Bis●Tris, 100 mM NaCl, 0.1 mM EDTA, 5 mM DTT, and 4% (wt/vol) anionic bicelles, pH 6.5.

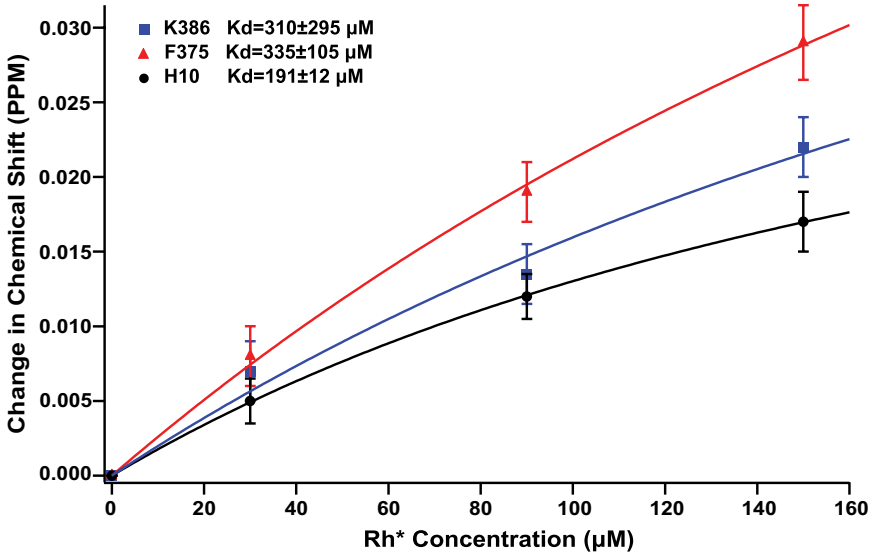

Fig. S7. Estimation of K_D for arrestin-1 binding to Rh*. The dose-dependent chemical-shift changes in arrestin-1 peaks positions (from Fig. S5) were plotted as a function of the concentration of Rh* for residues K386 (blue), F375 (red), and H10 (black). The K_D for each curve was determined by fitting the model for 1:1 noncooperative binding to the data using nonlinear least squares analysis (Eq. **S1**). The large uncertainties associated with two of three fits plus the fact that the lowest of the three K_D was determined to be larger than the higest Rh* concentration reached in the titration leads to the conclusion that K_D is very reliably determined to be larger than 0.15 mM by these data.

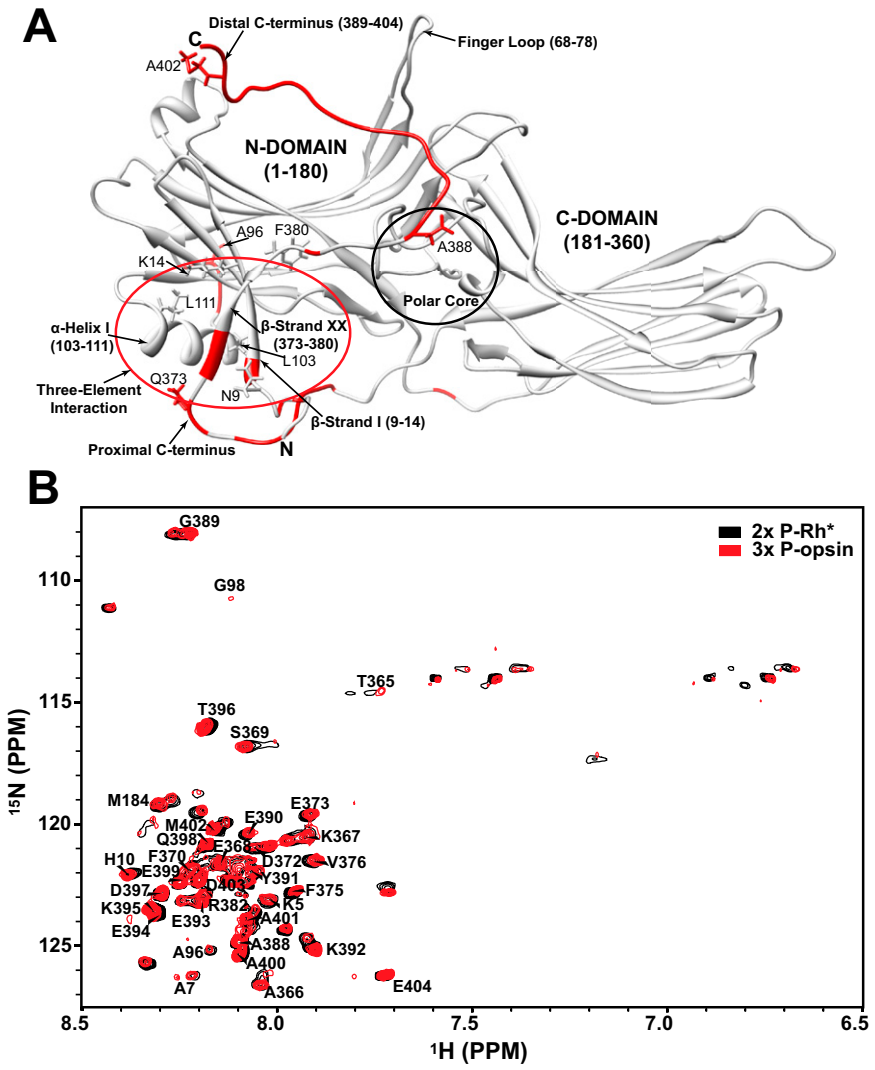

Fig. S8. (*A*) Location of sites in the arrestin-1 structure that yield visible TROSY NMR resonances following formation of a complex with P-Rh*. Red sites in the arrestin-1 structure (PDB ID 1CF1) are those for which resonances are observable in the TROSY NMR spectrum of arrestin-1 following complex formation with P-Rh* (Fig. 2*B*). (*B*) Comparison of the NMR spectrum for arrestin-1 complexed with P-opsin versus its spectrum when complexed with P-Rh*. The TROSY spectrum of 30 μM $^{2}H,^{15}N$-labeled arrestin-1 in the presence of 90 μM P-opsin is shown in red. Samples contained 25 mM Bis•Tris buffer, 100 mM NaCl, 0.1 mM EDTA, 5 mM DTT, 5 mM NH_2OH, and 4% (wt/vol) anionic bicelles pH 6.5. The spectrum was acquired at 308 K. The spectrum of 30 μM arrestin-1 in the presence of 60 μM P-Rh* (black) was collected under identical conditions.

Table S1. Impact of complex formation with P-Rh* on arrestin-1 PREs between spin-labeled residue 16 and the distal C terminus

Paramagnetic relaxation enhancement of resonances from the arrestin-1 C-tail

	No P-Rh*	3× P-Rh*
Residue	I_p/I_0	I_p/I_0
E404	0.21	1.02
D403	0.16	0.86
M402	0.07	0.97
A401	0.08	1.00
A400	0.11	1.04
E399	0.12	0.99
Q398	0.25	1.05
D397	0.25	0.92
T396	0.28	0.95
E393	0.28	0.98
K392	0.43	0.91
Y391	0.38	N/A
E390	0.49	0.89
G389	0.42	0.79
A388	0.52	0.79
K386	0.57	N/A
L385	0.44	N/A
N384	0.35	N/A
F380	0.00	N/A
E379	0.00	N/A
S369	1.01	0.81
K367	0.98	0.84
A366	0.96	0.9
T365	0.99	0.89
D364	1.00	0.78
D362	1.06	0.97
E361	1.07	0.98

Intensity ratios are given for each TROSY NMR peak under conditions where a nitroxide spin label is present (intensity = I_p) at residue 16 relative to conditions in which the spin label was converted to a diamagnetic form (intensity = I_0). Measurements were carried out for 30 μM arrestin-1 in bicelles in the absence or presence of 90 μM P-Rh* at pH 6.5 and 308 K. N/A: Measurement could not be made because peak intensity was too low under nonparamagnetic conditions.